Publishing House
AKAPIT

COMPUTER METHODS IN MATERIALS SCIENCE
Informatyka w Technologii Materiałów

Vol. 18, 2018, No. 2

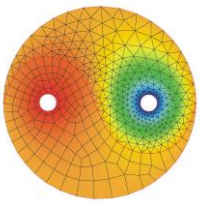

HEADING OF SMALL BI-METALLIC COMPONENTS FOR ELECTRIC CONTACTS

WOJCIECH PRESZ*, ROBERT CACKO

Institute of Manufacturing Technologies, Warsaw University of Technology, Narbutta 85, 02-524 Warsaw, Poland
**Corresponding author: w.presz@wip.pw.edu.pl*

Abstract

Electrical connectors mostly have silver contacts joined to the supplying and discharging electric current elements by riveting. In order to reduce costs, the rivet core of the contact can be replaced with a cheaper material such as copper. There is a wide range of commercially offered bi-metallic, silver-copper rivets available for the production of contacts. This generates a new situation in the riveting process, as the bi-metallic rivet is to be formed. In the analyzed example it is a small-sized object that places it near the limits of micro-forming. The riveting process was originally designed by classical upsetting. It was based on the results of FEM simulation taking into account the deformation of three materials included in the joint: two materials for rivet and sheet material. The FEM results were verified by the results of experimental studies indicating high compliance. The elimination method of the elastic deformations of the load system impact on the process forces was elaborated and it was used for comparative analysis with the force run obtained from FEM. The model simulating the working conditions of the connector was developed. Based on the joint load modeling results, the cause of possible delamination of constituent materials was determined. It was also defined the desired silver distribution in the connector head to eliminate the risk of separation of both materials during exploitation.

Key words: Metal forming, Heading, Bi-metallic component

1. INTRODUCTION

Growing interest in ecology, especially because of the worrying increase in air pollution, imply intensive interest in electrical devices improvement. A good example of this tendency is the issue of electro-mobility (Green e-motion project, 2016). On the other hand, progressive miniaturization is taking place, which also results in the emergence of new technologies such as, e.g., extracted in the area of metal forming – micro-forming (Geiger et al., 2001). This leads to a forecast of demand growth of electrical connectors, also miniaturized. In perspective of the further growth of mass production of contacts, the reduction of material costs in this sector is a potential source of large savings. One way to obtain that effect is to replace the silver contacts (figure 1a, Yueqing Hawin Electric Co., Ltd.) with the one with core made of a cheaper material with similar electrical properties, e.g. copper (figure 1b, Wenzhou Saijin Electrical Alloy Co., Ltd.). The market offers a wide range of dimensions of bi-metallic rivets, such as Ag-Cu, for electric connectors. Their structure consisted of two metals, creates a new conditions during the riveting process, in which both metals are deformed and a connector made of a third metal (figure 1c).

Methodology of micro-forming process design (Presz & Cacko, 2011; Olejnik et al., 2009), microjoining (Presz & Cacko, 2018a) and suitable microtools (Presz, 2016; Presz & Rosochowski, 2017) according to uniform materials have been presented in several articles. Bi-metallic components manufacturing analysis are presented to a lesser extent.

 ISSN 1641-8581

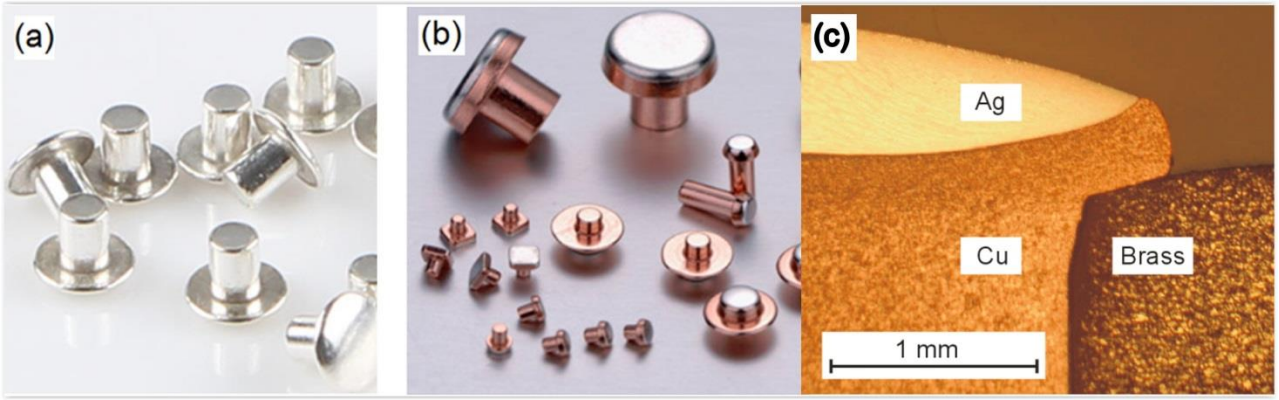

Fig. 1. *Electrical contact rivets: (a) solid - silver, (b) bimetallic – silver / copper, (c) cross-section of assembled bimetallic electric contact.*

During metal forming of bi-metallic components it is important to take into account the fact that each material may have different formability (resistance to plastic deformation), which usually varies – most often grows – while deformation progresses. This introduces additional design difficulties. Predicting the multi-flow of two materials (Kocanda et al, 1996) even in the case of relatively simple geometric processes, like upsetting (Essaa et al., 2012) or extrusion and forging (Kazanowski et al., 2004; Politis et al., 2012) is considered as accomplishment. The complexity of material flow with respect to bi-metallic components is a problem in modeling such processes. These difficulties increase with decreasing dimensions of objects due to occurrence of so-called scale effects (Geiger et al., 1997; Tiesler, 2002). They may be related with the internal structure (Raulea et al., 2001; Presz & Rosochowski, 2006) and contact phenomena (Chunju et al., 2014; Wang et al., 2014; Presz & Cacko, 2017; Muster & Presz, 1999). With component dimensions decrease, the surface layer contribution to deformation process becomes increasingly larger. The complexity of problems related with small bi-metal components forming causes the need for research to increase the accuracy of modeling such processes. The main aim of the research was to determine the mechanism and conditions for delamination with the numerical analysis support. Based on the obtained information (Presz & Cacko, 2018b), the adequate material distribution from the operational point of view was determined, which would prevent this delamination.

2. DESCRIPTION OF THE PROCESS

The bi-metallic connector riveting process was analyzed using the heading process (figure 2). The bi-metallic rivet exposed in figure 2a presents the two-side connector after assembling.

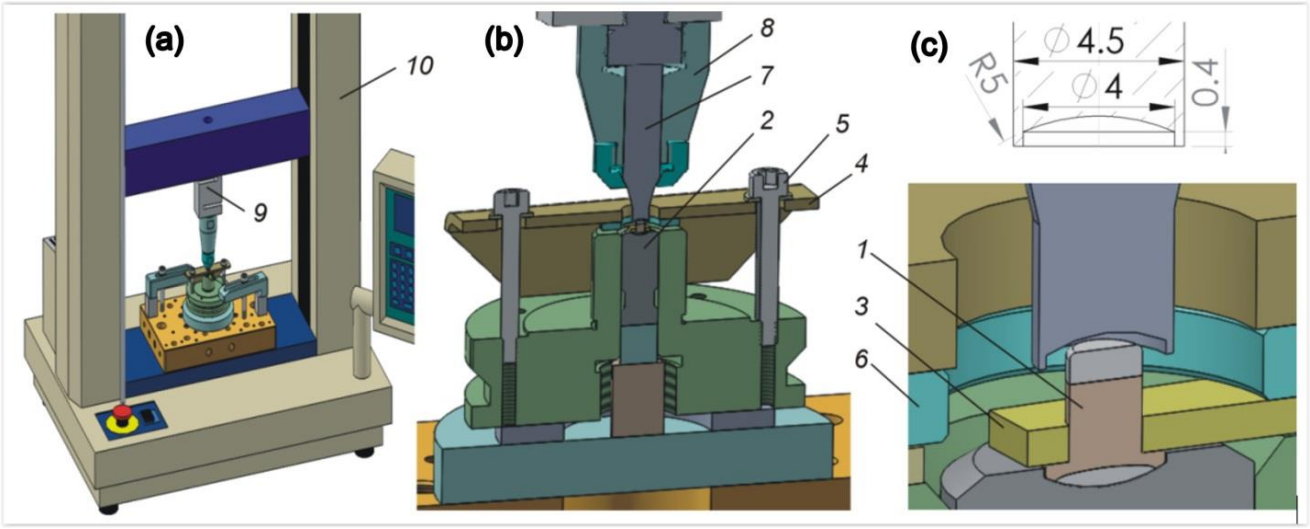

Fig. 2. *Experimental set-up (description in the text); a) the two-side connector after assembling, b) the process diagram with all components, c) the dimensions of the punch cavity and the die.*

The process diagram is shown in figure 2b. Bi-rivet (1) is placed in a cavity of the die (2), in frame (3), which is kept with the blank holder (4), with screws (5), through the washer (6). Heading is carried out with a punch (7) coupled via binding (8) of a force transducer (9) located on the beam of the precision Hounsfield HS10S strength machine. Heading is carried out at frame speed $V_r = 6.6\times10^{-5}$ m/s (4 mm/min) to the specified displacement. The deformed rivet forms a bi-side connector with silver contacts on both sides. For a comparison, a straightforward heading of the bi-metallic rivet was also carried out, which is shown in figure 3. The dimensions of the punch cavity and the die are identical (figure 2c).

2.1 Numerical modelling

Numerical model for the analysis has been prepared in two versions, reflecting laboratory tests procedure: actual two-head of the rivet shape forming, and one-head of the rivet forming. First model of the rivet forming process consists of eleven components (figure 3): four rigid parts – punch pusher (1), counter-punch pusher (2), two removers (3), four deformable, with only elastic properties zones – punch (4), counter-punch (5), holder (6), blocking sheet (7), and deformable rivet consisted of three zones (8) with elastic-plastic with strain hardening properties: left and right are silver made parts and inner is copper made part. The second model differs from the first one only by lack of blocking sheet, responsible for material flow forcing to form bottom head. Both models are static, axisymmetric and isothermal. Four-node 2D finite elements with axisymmetric properties have been used for meshing all deformable areas. High local stress/strain gradients required usage of remeshing procedure, which – as usual – have needed initial optimization.

Tool parts – punch, counter-punch, holder and remover – are assumed to be made of tool steel and elastic properties are only applied in form of Young modulus, E = 210 000 MPa, and Poisson's ratio ν = 0.31 for these parts of the model. For all surfaces friction coefficient μ = 0.25 was assumed except rivet copper-silver contact zones, were glue option with stress threshold was applied. Materials for the contact, which were brass M63, silver 930 and copper M1, were modelled using elastic-plastic material model with hardening. Based on stress-strain curves published (Stress-Strain Curves, 2002), data for numerical analysis according to Huber-Mises yield criterion were determined, and are collected in table 1.

Table 1*. Data used for material description in numerical modeling.*

Material	Stress– strain curve	Young modulus, MPa	Poisson ratio
Copper (M1)	$\sigma_p = 390\ \varepsilon^{0.3}$	107 000	0,33
Brass (M63)	$\sigma_p = 710\ \varepsilon^{0.48}$	145 000	0,32
Silver (930)	$\sigma_p = 375\ \varepsilon^{0.25}$	70 000	0.37

2.2 Experimental results

As a result of the experiment, the accurate contact shown in figure 4a, labeled as locked heading (L) have been successfully made. For a comparison purpose the rivet after upsetting, labeled as free heading (F) showed in figure 4b, has been completed and evaluated in accordance to the final aim – properly headed contact (figure 4c). The geometry of analyzed processes were controlled (figure 4d), and forces of both processes were also recorded and compared with results from numerical analysis.

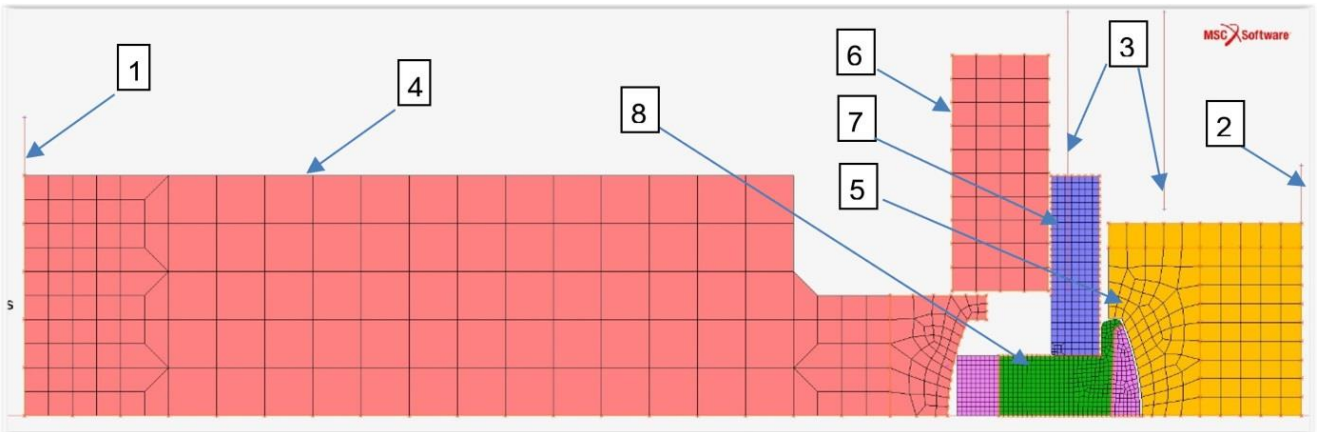

Fig. 3. *Both rigid and deformable parts of FEM model – description in the text.*

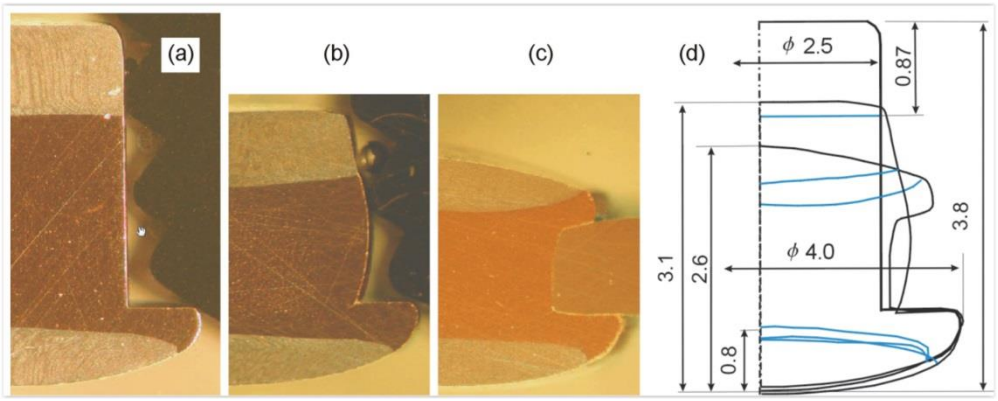

Fig. 4. *Locked (a) and Free (b) heading results, both side heading (c), the main dimensions of locked, free and both side heading.*

3. ANALYSIS OF THE RESULTS

The flow of the locked heading process was considered first. The model consisted of seven parts: A and C are silver, B – copper, D – brass, and E, F, and G are improved tool steel (figure 5a). The deformation of all the elements, except for the blankholder G, affects the final shape of the contact, however, to a different degree. The deformations of tools E and F have a little effect and may be omitted in the analysis. The impact of the remaining A, B, C and D is significant. Moreover, during the process they interact with each other. The rivet is placed in the die and a frame is applied to support it, which is then pressed by the holder. In places shown with arrows on figure 5a, there are clearances – CL. The upsetting process starts, initially resulting in uneven flow of material in A and B zones (figure 5b) arrow, and at the later stage similarly zones C and D. Additionally all clearances CL are eliminated (figure 5c).

It has to be noted, that the frame D is bent and its hole becomes deformed – dotted lines in figures 5c and 5d. This is an important detail – especially in case of micro-components – since the enlarged hole in the frame takes away part of the material, which forms the upper part of the contact. If the frame D become too big, the correct shape of the joint could not be achieved. Parts A and B continue to deform non-uniformly to create a concavity at the contact surface of the two materials and part A penetrates part B to a greater depth (figure 5d). The material of part B is pressed outside, reaches the wall of punch cavity (figure 5e), and changes its flow direction, causing the alignment of undesired concavity (figure 5f). After opening the work space (figure 5g), process is completed by the contact of the expected shape. As a comparison, there is also final result of FEM simulation of the free headed contact presented in the figure 5h, corresponding with the shape obtained experimentally, shown in figure 4b.

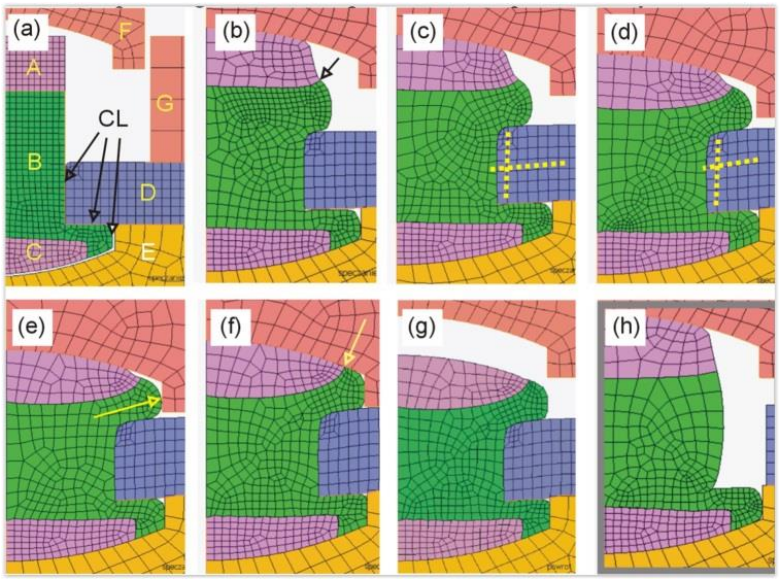

Fig. 5. *Locked heading process – numerical modeling results: a) silver parts of contact (A, C), copper part (B), brass part (D), lower (E) and upper (F) punches, blankholder – G; b) uneven flow of material at initial stage of upsetting; c) clearances elimination; d) parts A and B greater depth penetration; e) material of part B reaches the wall of punch cavity; f) material flow direction causing the alignment of concavity; g) opening the work space; h) final contact shape after simulation.*

3.1 Free heading process

This process was conceived as a reference to the locked heading process, giving opportunity to verify FEM modeling parameters. The subject of the analysis was the strength of the process, the outline of the deformed object – especially at the point of connection between the two materials and the distribution of these materials on the cross section. The successive stages of the upsetting process and the deformation distribution in the final phase are presented in figure 6. The outline of the FEM simulation (figure 6c) was laid on the shape marked as out which is the contour of the deformed cross section taken from figure 4b. The outline of the FEM simulation is similar to the outline of a metallographic section. Also the separation lines of both materials in the FEM simulation and the result of the experiment are consistent.

3.2 Process force

The recorded forces of the process are superposition of the deflection of the elastic parts of the machine and the tooling. Because of the small size of the object, these deflections significantly affect the course of the recorded forces and should be taken into account. The elastic deflection of the machine, tools and tooling was eliminated in comparison between the FEM and experimental results. This was done on the basis of the course of unloading forces. In case of experimental forces, the unloading functions were approximated by linear functions in three intervals determined by the distinct changes in slope of the unloading curves. The procedure is explained in the example of the process flow F (Free upsetting, figure 7b, c). The unloading force was approximated in the three ranges of measuring points < s, a), < a, b) and < b, n) with three straight lines with the directional coefficients k_1, k_2, and k_3 shown in the drawing. Local component of correction because of the elastic deflection corresponding to the point i (i = 0 at point s) is given by:

$$\delta x_i = \begin{cases} \delta^a x_i = \dfrac{Y_i - Y_{i-1}}{k_1}, & i = 1,2\ldots,a \\ \delta^b x_i = \dfrac{Y_i - Y_{i-1}}{k_2}, & i = a+1, a+2\ldots,b \\ \delta^n x_i = \dfrac{Y_i - Y_{i-1}}{k_3}, & i = b+1, b+2\ldots,n \end{cases} \tag{1}$$

where: Y_i – recorded process force corresponding to the measuring point i, $k_{1,2,3}$ – the directional coefficients of the lines approximating the relief, $\delta^{a,b,n}x_i$ – local components of correction because of elastic deflection.

The elastic correction of the position of the point corresponding to the process force is equal to the sum of all components of the elastic corrections up to the considered force point and is given by the following formula:

$$\Delta_i = \begin{cases} \Delta^a x_i = \sum_{i=1}^{a} \delta^a x_i, & i = 1,2,\ldots,a \\ \Delta^b x_i = \Delta^a x_a + \sum_{i=a+1}^{b} \delta^b x_i, & i = a+1, a+2,\ldots,b \\ \Delta^n x_i = \Delta^a x_a + \Delta^b x_b \sum_{i=b+1}^{n} \delta^n x_i, & i = b+1, a+2,\ldots,n \end{cases} \tag{2}$$

where: $\Delta^{a,b,n}x_i$ – corrections of displacement positions due to elastic deflection for three analysed ranges.

The recorded process force, which is a set of measuring points after the modification consisting of accounting for the elastic correction, is transformed into a set according to the equation:

$$\begin{aligned} & F = \{(x_i, Y_i), i = 1,2,\ldots,n\} \\ & \underset{mod}{\rightarrow} \quad F_{mod} = \{(x_i - \Delta_i, Y_i), i = 1,2,\ldots,n\} \end{aligned} \tag{3}$$

where: F – set of measured points, F_{mod} – set of points taking into account the correction due to elastic deformations of the load system (machine, tools and tooling).

The modification method described above has been applied to registered process forces and FEM results. Experimental L and F runs as well as Lmod and Fmod adjusted runs are shown in figure 7c. The intervals to which further directional coefficients relate are also marked. The same procedure was performed with respect to FEM results. There, in turn, was a slight spring deflection of the tools.

Run marked as L-FEM and F-FEM and modified L-FEM-mod and F-FEM-mod are presented in figure 7d. Comparison of modified experimental results and numerical modeling is shown in figure 7e. Compatibility of results should be considered satisfactory, taking into account the fact of up to three plastically deformable materials interaction, for which elastic-plastic with hardening models are applied.

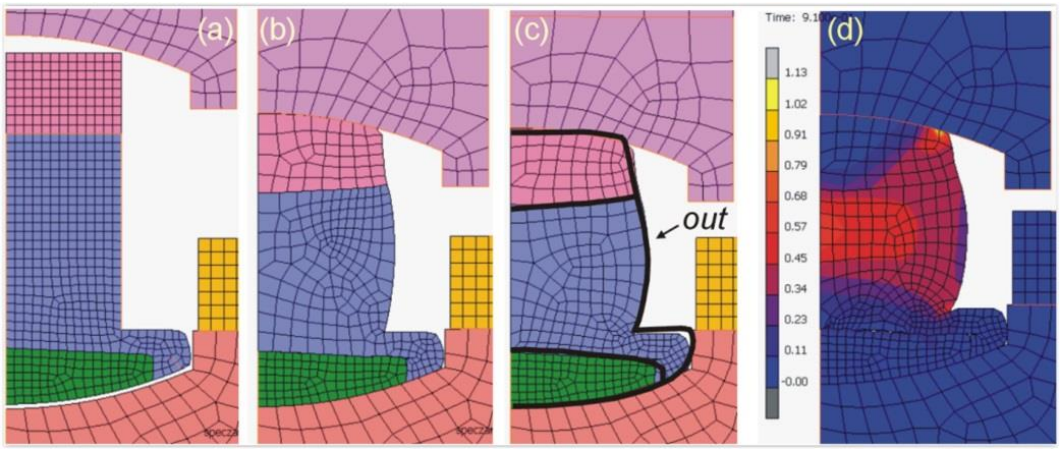

Fig. 6. *Simple upsetting process of bimetallic components performed as an reference process for the main FEM model verification.*

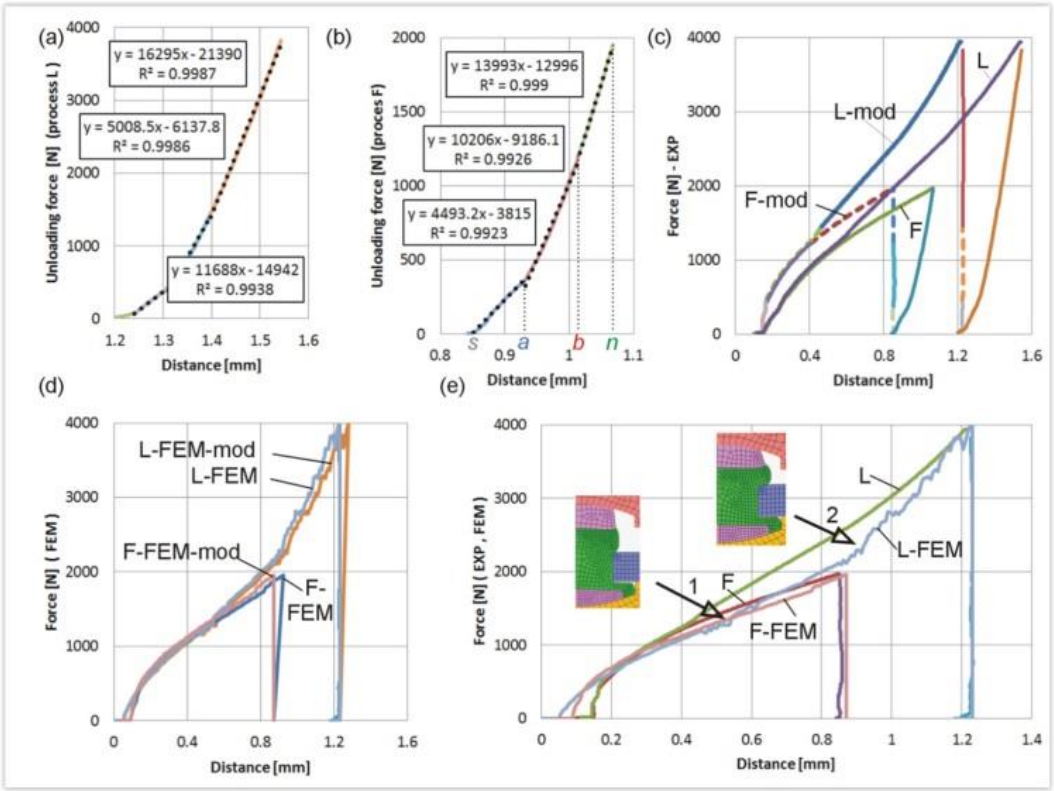

Fig. 7. *Simple upsetting process of bimetallic components performed as an reference process for the main FEM model verification.*

The biggest differences occur in points 1 and 2, in which the increase of the process force obtained from FEM simulation changes the intensity. This phenomenon was not observed in the experimental plot. The phase images of the process corresponding to points 1 and 2 do not suggest the reason for the differences. This issue needs explanation in further studies.

4. REQUIRED HEAD STRUCTURE OF BIMETALLIC CONTACT RIVET

The FEM model included simplified working conditions of bimetallic riveted contact with the material distribution obtained by FEM simulation. This distribution has been verified experimentally. The load process was carried out in the same model immediately after the riveting process – the stress and strain distribution remaining after riveting were retained. The strains induced for research purposes significantly exceed the deformations expected during operation, however, allow easier tracing of the direction of changes progressing during contact operation. The following loading phases during numerical modeling are shown in figures 8 and 9, for type A and B respectively.

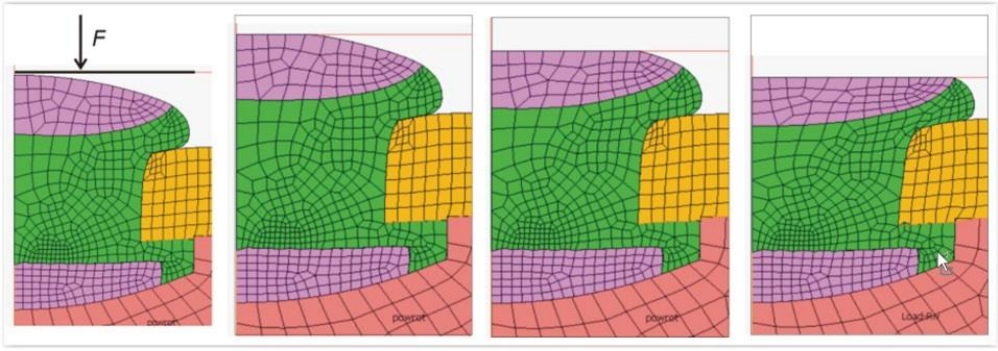

Fig. 8. *Loading of a bimetallic contact rivet type A.*

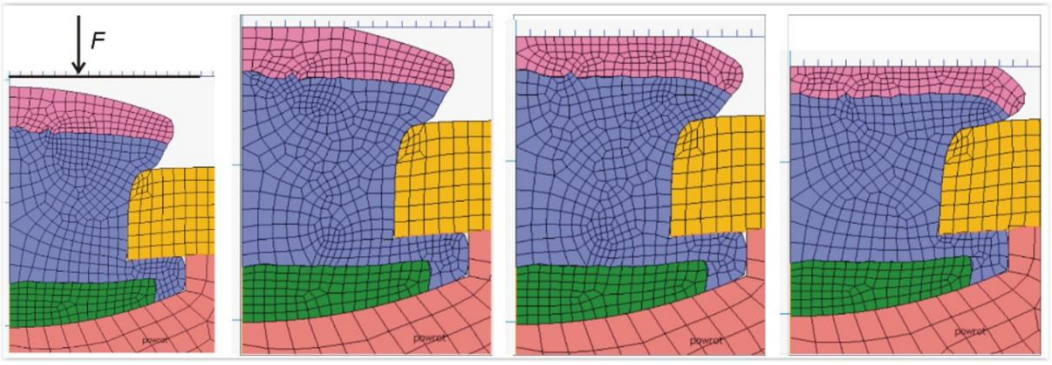

Fig. 9. *Loading of a bimetallic contact rivet type B.*

The additional mechanical coupling of the silver and copper areas created during the heading not only does not deteriorate but also has a tendency to develop. It is illustrated in figure 9. The silver area, in each of the phases of the load, is surrounded by the copper area. Contact loading results in penetrating the silver layer into the core of the copper core. This is presented in figure 10, showing the flow vectors of both materials, which directions are convergent. This situation virtually excludes the risk of separation of both materials, which is the main potential destructive mechanism.

5. CONCLUSIONS

- A simple bimetallic riveting process was designed, carried out and modeled. This process was used for initial verification of further models. Good consistency of process forces and material distribution in the volume of the rivet was obtained.
- A numerical model of the deformation of a system consisting of three metals: silver, copper and brass was developed, creating a bimetallic contact. Good consistency of modeled process forces and shapes was obtained.
- A method for considering the elastic deflection of the load system for micro objects has been developed. The use of this method allows for precise comparison of experimentally determined forming forces with the results of numerical modeling. The method eliminates the need to model the machine and the tooling system, which elastic deflections significantly affect the force run.

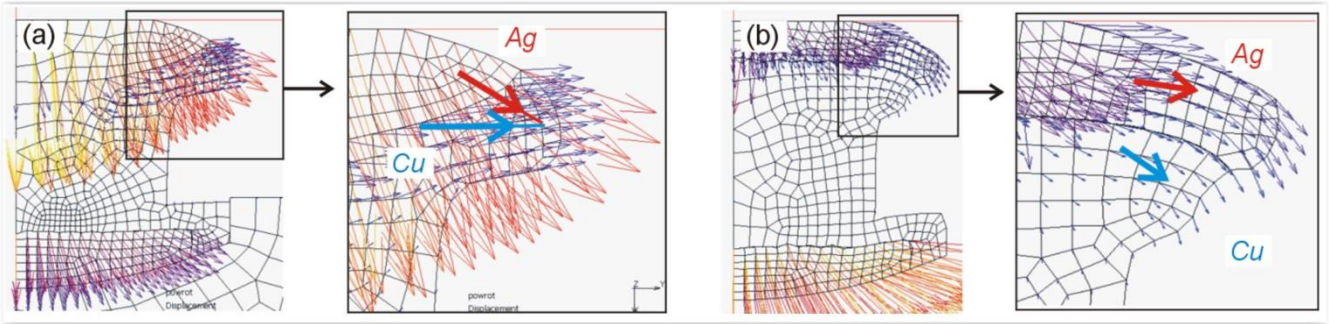

Fig. 10. *Displacement vectors during loading test of bimetallic ribet contacts: (a) type A, (b) type B.*

- The FEM model simulating the work of the obtained joint was developed.
- The process of riveting of small bimetallic contact was successfully carried out in laboratory scale, obtaining a favorable distribution of materials from the point of view of operational loads.
- Based on the FEM experiment, it was demonstrated that the silver distribution in the head obtained during the riveting process ensures the stability of the connection with the copper during operation. This means that the main threat of damage to the bimetallic contact that is the separation of both materials was eliminated.

REFERENCES

Essaa, K., Kacmarcik, I., Hartley, P., Plancak, M., Vilotic, D., 2012, Upsetting of bi-metallic ring billets, *Journal of Materials Processing Technology* 212, 817- 824.

Geiger, M., Kleiner, M., Eckstein, R., Tiesler, N., Engel, U., 2001, Microforming, *CIRP Annals – Manufacturing Technology*, 50 (2), 445-462.Geiger, M., Messner, A., Engel, U., 1997, Production of microparts – Size effects in bulk metal forming, similarity theory, *Production Engineering*, 4, 55-58.

Green e-motion project, 2016, *Paris Declaration on Electro Mobility and Climate Change & Call to Action*; www.greenemotion-project.eu

Kazanowski, P., Misiołek, W.Z., Epler, E.E., 2004, Bi-metal rod extrusion—process and product optimization, *Materials Science and Engineering*, A369, 170-180

Kocanda, A, Presz, W., Mazurek, W., Adamczyk, G., 2001, Contact pressure distribution in upsetting of compound metals, *Journal of Materials Processing Technology*, 60, 44-48.

Muster, A., Presz, W., 1999, Influence of initial surface roughness on galling behavior of steel-steel couple, *Scandinavian Journal of Metallurgy*, 28 (1), 5-8.

Olejnik, L., Presz, W., Rosochowski, A., 2009, Backward Extrusion using Micro-Blanked Aluminium Sheet, *International Journal of Material Forming*, 2, 1, 617-620.

Paris Declaration on Electro Mobility and Climate Change & Call to Action, 2015, Lima – Paris.

Politis, D.J., Lin, J., Dean, T.A., Balint, D.A., 2014, An investigation into the forging of Bi-metal gears, *Journal of Materials Processing Technology*, 214, 2248– 2260.

Presz, W., Cacko, R., 2011, Influence of Micro-Rivet Manufacturing Process on Quality of Micro-Joint, *Proc. 14th Int. Conf. on Material Forming, Esaform 2011*, Belfast, American Institute of Physics Conf. Proc. 1353, 1, 541-546.

Presz, W., Cacko, R., 2017, Ultrasonic assisted microforming, *26th Int. Conf. on Metallurgy and Materials, METAL*, Brno, 2017, 521-526

Presz, W., Cacko, R., 2018a, Bimetallic Micro-Punches for Micro-Blanking Processes, *Archives of Metallurgy and Materials*, 63, 29-34.

Presz, W., Cacko, R., 2018b, Determination of material distribution in heading process of small bimetallic bar, *AIP Conference Proceedings*, 1960, 050014.

Presz, W., Rosochowski, A., 2006, The influence of grain size on surface quality of microformed components, The 9th *Proc. Int. Conf. on Materials Forming, ESAFORM 2006*, Glasgow, 587-590.

Presz, W., Rosochowski, M., 2017, Application of semi-physical modeling of interface surface roughness in design of pre-stressed microforming dies, Int. Conf. on the Technology of Plasticity, ICTP 2017, *Procedia Engineering*, 207, 1004-1009.

Presz, W., 2016, Scale effect in design of the pre-stressed micro-dies for microforming, *Computer Methods in Materials Science*, 16, 196-203.

Raulea, L.V., Goijaerts, A.M., Govaert, L.E., Baaijens, F.P.T., 2001, Size effect in the processing of thin metal sheets, *Journal of Materials Processing Technology*, 115, 44-48.

Stress-Strain Curves, 2002, Material Park, OH 44073-0002.

Tiesler N., 2002, Microforming - Size effects in friction and their influence on extrusion processes, *Wire*, 52, 1, 34-38.

Wang, Ch., Guo, B., Shan, D., Zhang, M., Bai, X., 2014, Tribological behaviors in microforming considering microscopically trapped lubricant at contact interface, *Journal of Advanced Manufacturing Technology*, 71, 2083-2090.

Yueqing Hawin Electric Co., Ltd., https://hawin.en.alibaba.com/.

Wenzhou Saijin Electrical Alloy Co., Ltd., https://saijinele.en.alibaba.com/

SPĘCZANIE MINIATUROWYCH BIMETALICZNYCH ELEKTRYCZNYCH KONTAKTÓW

Streszczenie

Łączniki elektryczne w dużej części posiadają srebrne styki łączone z elementami doprowadzającymi i odprowadzającymi prąd elektryczny metodą nitowania. W celu obniżenia kosztów trzon nitu będącego stykiem można zastąpić materiałem tańszym, jakim jest miedź. Na rynku istnieje szeroki zakres wymiarowy komercyjnie dostępnych srebrno-miedzianych nitów z przeznaczeniem do produkcji styków. Stwarza to nową sytuację w procesie nitowania, ponieważ nitowaniu ulega obiekt bimetaliczny. W analizowanym przykładzie jest to obiekt o niewielkich rozmiarach, które umieszczają go na granicy mikroformowania plastycznego. Wstępnie zaprojektowano proces nitowania metodą klasycznego spęczania. Oparto się na wynikach symulacji MES uwzględniającej odkształcenia trzech materiałów wchodzących w skład złącza: dwóch materiałów nitu i materiału blachy. Wyniki MES zweryfikowano wynikami badań doświadczalnych uzyskując dobrą zgodność. Opracowano metodę eliminacji wpływu odkształceń sprężystych systemu obciążenia na przebieg rejestrowanych sił procesu i zastosowano ją do analizy porównawczej z przebiegami sił uzyskanymi z symulacji MES. Opracowano model symulujący warunki pracy złącza. Na podstawie wyników modelowania obciążenia złącza wykazano, że uzyskany rozkład srebra w główce złącza eliminuje zagrożenie rozdzieleniem obu materiałów w trakcie eksploatacji.

Received: January 25, 2018
Received in a revised form: May 14, 2018
Accepted: December 27, 2018